Polym. Bull.
DOI 10.1007/s00289-016-1839-4

ORIGINAL PAPER

Long-chain branched polypropylene obtained using an epoxy resin as crosslinking agent

Jorge Guapacha[1] · Enrique M. Vallés[1] · Lidia M. Quinzani[1] · Marcelo D. Failla[1,2]

Received: 3 December 2015 / Revised: 18 August 2016 / Accepted: 21 October 2016

Abstract A reaction between a linear polypropylene functionalized with maleic anhydride (PPg) and epoxy resin (bisphenol A diglycidyl ether) was carried out on the molten state to generate long-chain branches (LCB) in the molecular structure of the PPg. Concentrations of epoxy resin (ER) of up to 3.15 wt% were employed to obtain different levels of branching. FTIR spectroscopy analysis indicates that during the reaction, anhydride groups in PPg are consumed and new ester groups are formed. The presence of branches was verified using multiple-detection size-exclusion chromatography and rheology. The degree of long-chain branching induced in PPg augments with increasing concentration of ER. Furthermore, the materials modified with higher content of ER display gel-like behavior. The long-chain branched polymers also display thermo-rheological complexity. Thermal characterization studies show that LCBs have a nucleating effect during crystallization and cause the augment of the crystallization activation energy of PPg.

Keywords Polypropylene · Crosslinking · Structure–property relations · Rheology · Calorimetry

Introduction

The industrial synthesis of polypropylene (PP) produces highly linear stereospecific polymers with many excellent properties, such as low density, high melting temperature, and good mechanical and chemical resistance. These features make PP

✉ Lidia M. Quinzani
lquinzani@plapiqui.edu.ar

[1] Planta Piloto de Ingeniería Química (PLAPIQUI), UNS-CONICET-C. C. 717-(8000), Bahía Blanca, Argentina

[2] Departamento de Ingeniería, Universidad Nacional del Sur (UNS), Av. Alem 1253-(8000), Bahía Blanca, Argentina

Published online: 26 October 2016

useful for many applications in the automotive industry, food packaging, structural support and a broad range of products from day to day life. However, its performance is not suitable for processes that require good melt strength and strain hardening such as thermoforming, foaming, blow molding, film molding and fiber spinning [1, 2]. To be able to use PP in those processes, melt strength and strain hardening must be enhanced. This can be done by blending the PP with polymers with good extensional properties, such as like low-density polyethylene [3], by including a fraction of high molecular weight PP, or by introducing long-chain branches (LCB) in the linear backbone of the PP molecules. This last method is the most efficient mechanism to improve the melt strength and strain hardening [4–22]. The presence of LCBs increases the terminal relaxation time enhancing the melt strength and improving the strain hardening behavior of the material in extensional flows [5, 7, 9–11, 14, 15, 17, 20, 22, 23].

Nowadays, important advances in the procedures for synthesizing PP with LCB have been done. These strategies can be grouped into two groups. The first one seeks to generate the LCB during the polymerization reaction [12, 13, 17, 24]. In the other group, the modification is carried out during a post-polymerization stage that takes place after the main polymerization of a conventional linear PP. This later approach has gained large attention for its versatility. There are several forms to accomplish the post-polymerization modification, such as irradiation, [5, 9, 10, 15, 25, 26] solid-state grafting, [7] and reactive extrusion. In this last case, PP is processed in the molten state in the presence of organic peroxide and a multi-functional monomer. The peroxide attacks the PP molecule producing macroradicals that react with the monomer generating LCB in PP [4–6, 8, 11, 14, 16, 19–22, 27]. This process can be also applied to a functionalized PP such as maleic anhydride grafted PP (PPg). In this case, no peroxides are needed and the branching reaction is achieved using different multi-functional monomers that react with the anhydride groups [18, 22, 28, 29].

Following a previous study in which glycerol was used as a chain-branching agent [22], in the present work, long-chain branched PP (PPr) is obtained by melt processing a commercial PPg in the presence of diglycidyl ether of bisphenol A (DGEBA). Tang and coworkers [28] used DGEBA, as well as two other epoxi resins, to introduce LCB in 50:50 PP/PPg mixtures using reactive extrusion at 190 °C. The PPg they use is obtained in an early stage by grafting maleic anhydride into the PP. They observe that the melt flow rate decreases and the sagging resistance of the polymer greatly improves with the presence of the LCBs.

In this paper, infrared spectroscopy (FTIR) is used to verify the extent of the branching reaction and high-temperature size-exclusion chromatography (SEC) to evaluate the changes in molecular weight distribution and to estimate the amount of long-chain branching induced on the polymer chains. The branched polypropylenes are also characterized using small-amplitude oscillatory shear flow and differential scanning calorimetry (DSC).

Experimental

Materials

A PPg from Uniroyal Chemical Co. (Polybond 3200, $M_w = 120$ kg/mol and $M_w/M_n = 2.6$) is used in this work. Since this polymer was provided partially hydrolyzed, it was kept at 130 °C under vacuum for 8 h before used. The amount of anhydride groups (AG) in the treated PPg was determined by FTIR as 0.74 wt% following the methodology described in the Results and Discussions Section. The crosslinking agent is an epoxy resin (ER), the diglycidyl ether of bisphenol A (D.E.R 332 from Dow Chemical). It was used as purchased.

Modification of PPg

The reaction between PPg and the ER was carried out in a Brabender Plastograph® mixer at 190 °C for 15 min using cam-blades rotating at 40 rpm. The unreacted ER was removed from the modified polymer by dissolving the materials in xylene at 120 °C under constant stirring in a nitrogen atmosphere. The polymer was then precipitated using methyl ethyl ketone at ~5 °C, and dried at 80 °C for 48 h under vacuum. The modified PPgs are identified as PPgE# where # is representative of the weight percentage of ER used in the modification. This percentage ranges from 0.65 to 3.15 wt% (see Table 1).

Characterization

The changes in the molecular structure of PPg were determined by analyzing the FTIR spectra recorded using a Nexus spectrophotometer from Nicolet. The spectra were obtained on ~100-μm-thick films in the range 400–4000 cm^{-1} using a resolution of 4 cm^{-1}. Each spectrum corresponds to the accumulation of 100 scans. The molecular parameters such as weight molecular weight (M_w), number average molecular weight (M_n) and degree of branching (N_{LCB}) of the polymers were estimated by SEC at 135 °C using a Viscotek 350 system from Malvern provided with three detectors: light scattering (LS), refraction index and online viscometer. The chromatograph was equipped with a set of PLgel 10-μm Mixed-B LS columns (Polymer Labs) and 1,2,4-trichlorobenzene containing 0.1 wt% of butyl hydroxyl toluene was used as solvent. The system was calibrated with polystyrene standards (Viscotek).

Table 1 Molecular parameters of PPg and the modified polymers

	Weight % of ER added	Mass recovery (%)	M_n (kg mol^{-1})	M_w (kg mol^{-1})	M_w/M_n
PPg	0	100	48.6	132	2.7
PPgE07	0.65	100	58.0	175	3.0
PPgE1	1.01	100	80.0	514	6.4
PPgE2	1.89	98.4	73.3	315	–
PPgE3	3.15	86.8	62.4	389	–

The elastic and viscous moduli of the polymers were determined using small-amplitude oscillatory shear flow in an *AR-G2* rheometer from *TA Instruments* equipped with 25-mm-diameter parallel plates. The samples used in the rheological tests were prepared by compression molding at 180 °C. The linear viscoelastic behavior of the different polymers was studied at 180 °C, at frequencies between 0.01 and 100 s^{-1}, applying a constant shear stress of 10 Pa. Stress sweeps were applied to all materials to select the conditions to apply in the frequency sweeps so that the rheological measurements were well in the linear viscoelastic range of each polymer. The thermo-rheological behavior of the PPrs was also analyzed by measuring the dynamic moduli at temperatures between 173 and 201 °C.

A *Pyris 1* calorimeter from Perkin Elmer Co was used to study the thermal behavior using 20 mL/min of nitrogen flow. To erase the thermal history of the polymeric samples, they were heated up to 180 °C and held at this temperature for 3 min before cooling to 30 °C at different cooling rates (2.5–20 °C/min). Finally, they were heated again up to 180 °C at a rate of 10 °C/min. The crystallinity of PPg and modified polymers was determined from the heat of fusion measured in this last scan.

Results and discussion

Molecular characterization

During the melt processing of PPg in the presence of the ER, some of the AGs of the PPg react with the monomer generating esters links between the resin and the polymer [30]. An LCB is produced when an ER molecule reacts with at least two AGs belonging to different macromolecules. In this way, as the concentration of ER increases, the amount of remaining AGs should decrease while the concentration of ester groups increases. Figure 1 shows two regions of the FTIR spectra of PPg and

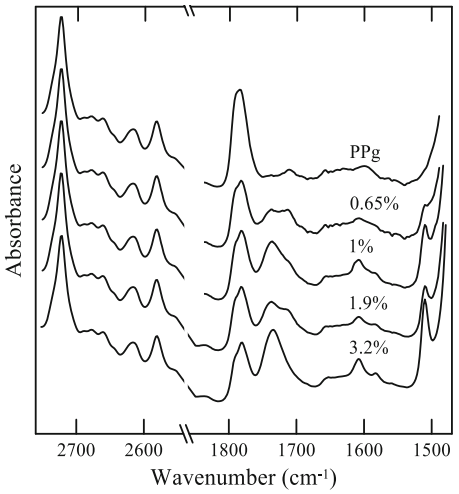

Fig. 1 FTIR spectra of PPg and the materials modified with different concentration of ER (shown next to each *curve*)

the modified polymers that allow the evaluation of the extent of the esterification reaction. The spectra were normalized using the absorbance of the signal at 2720 cm^{-1}, which corresponds to the methyne groups of PP. All the spectra display absorption bands at 1792 and 1860 cm^{-1} corresponding to the symmetrical and asymmetrical C=O stretching of anhydride. The PPgEs also present bands at 1715 and 1735 cm^{-1} that can be assigned to the stretching of carbonyls of acid and ester groups, respectively. In addition, absorbance bands located at about 1510 and 1610 cm^{-1} appear in the PPgE spectra which can be associated with the presence of aromatic rings from the ER [31]. The progressive decay of the peak corresponding to the AG and the growth of the bands associated with the reaction between the PPg and ER, both confirm that the resin is incorporated into the macromolecular structure.

The ratio of the absorbances at 1792 and 2720 cm^{-1} (A_{1792}/A_{2720}) can be used to estimate the remaining concentration of AGs in the modified polymers, through the calibration curve

$$\frac{A_{1792}}{A_{2720}} = 1.30 \times \text{wt\% AG} \tag{1}$$

This equation was obtained measuring the absorbances of physical mixtures of succinic anhydride with PP in concentrations ranging from 0.2 to 3 wt% [22]. The weight percentage of remaining AGs in each polymer, estimated with Eq. (1) using the A_{1792}/A_{2720} ratios, is shown in Fig. 2 as a function of concentration of ER. This figure also includes the ratio between the absorbance at 1735 and that at 2720 cm^{-1}, which is proportional to the amount of ester groups incorporated in PPr.

According to the data in Fig. 2, at low concentrations of ER, the amount of AGs rapidly decreases while the PPrs obtained with more than about 0.7 wt% of ER display similar amount of unreacted AGs. On the contrary, according to the ratio A_{1735}/A_{2720}, the ester groups rapidly augment at low concentrations of ER followed

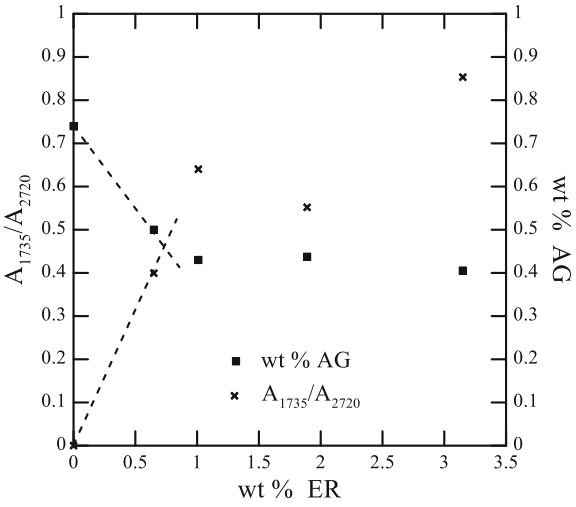

Fig. 2 Ratio of absorbances A_{1735}/A_{2720} (*left*) and concentration of remaining AGs (*right*) as a function of the concentration of epoxy resin

by a slower increase at higher concentrations. The constant value of unreacted AGs of about 0.43 wt% indicates that only ~40% of the original amount of AGs in PPg is consumed, regardless of the amount of ER used. Then, an average of 1.5 AG per molecule reacts irrespective of the amount of ER employed in the modification reaction, considering that an average of 3.6 AG is expected per original PPg macromolecule according to the amount of 0.74 wt% of AGs in PPg. Two reasons may explain this behavior, the inaccessibility of the remaining AGs when one or more of these groups in a PPg molecule have already reacted, and/or a possible phase separation of PPg and DGEBA. In this last case, the addition of ER above a given concentration may not be available to react with the Ags of PPg. Furthermore, the fact that the ratio A_{1735}/A_{2720} keeps increasing while the concentration of AG remains constant (after ~1 wt% of ER) may be due to formation of new ester groups through the reaction of ER with the acid groups already formed from the reacted AG. This is also suggested by the relative values of the absorbances at 1715, 1735 and 1610 cm^{-1} in the spectra of Fig. 1, which correspond to carbonyls of acid, ester and aromatic ring, respectively.

SEC coupled with triple detectors was used to determine the molecular weight distribution and corresponding average molecular weights, as well as to verify the presence of non-linear molecular structures in the polymers. A value of $dn/dc = 0.098$ ml/g was estimated for complete mass recovery of PPg, and later used to analyze the chromatograms of all PPrs. It must be mentioned that a noticeable amount of polymer was retained by the filtration system of the SEC equipment when characterizing the PPgEs obtained with 1.9 and 3.2 wt% of ER. The percentage of mass recovery estimated for each polymer is reported in Table 1. This result suggests that existence of very high molecular weight or gel-like material in an amount that increases with ER concentration.

Figure 3 shows all the normalized chromatograms of the light scattering detector at 90°. The detector at 7° gave equivalent signals, not reported here. The modified materials exhibit two clearly differentiated molecular populations while PPg has a typical chromatogram of a polymer with a Gaussian distribution of molecular

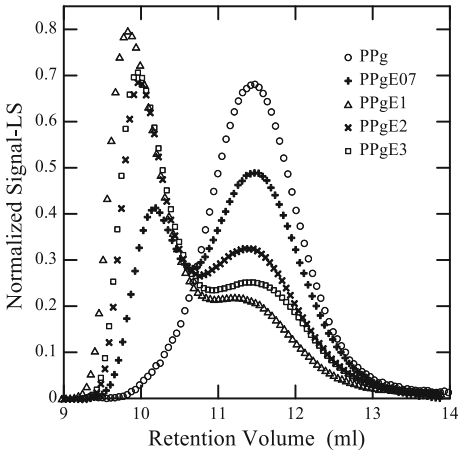

Fig. 3 Light scattering signal corresponding to PPg and the modified polymers (normalized with the area)

weights. One of the peaks displayed by the PPgEs is located about the same retention volume as the one corresponding to PPg, which it is surely constituted by PPg molecules. The other peak, which appears at smaller retention volumes, is formed by new macromolecular species of larger molecular weight. Polymers PPgE07 y PPgE1 show a gradual decrease of the PPg population with ER concentration and a corresponding gradual increase of high molecular weight material. The two materials modified with larger concentrations of ER (PPgE2 and PPgE3) display a different behavior. The peak at high retention volumes is higher than that of PPgE1 while the one at low retention volumes is lower. This pattern is due to the retention of highly crosslinked material that, as it was commented above, is filtered by the SEC system. Consequently, the chromatograms of PPgE2 and PPgE3 represent only the molecular weight distribution of the soluble portion and not the total mass of the modified polymer.

The molecular weight distributions of PPg and the PPgEs calculated from the information from all three SEC detectors are displayed in Fig. 4. The obtained distributions are consistent with the chromatograms of Fig. 3 already discussed. It can be observed that all PPgEs present a fraction at molecular weights larger than 10^6 g/mol, which is not present in PPg. This fraction increases with the amount of ER used in the modification process, PPgE1 being the material that shows the largest relative fraction. The high molecular weight material filtered in the case of PPgE2 and PPgE3 largely affects the displayed distributions. The shape of the distribution in the vicinity of 10^7 g/mol suggests that even a fraction of PPgE1 may be filtered by the SEC system. It has to be taking into account that the distribution curves are influenced by the value of d*n*/d*c* used to perform the calculations. The modification in molecular structure due to the crosslinking process may affect this value. Table 1 displays the number and weight average molecular weights calculated from the data in Fig. 4. The maximum values in molecular weight and polydispersity are obtained for the PPgE1. The high molecular weight material retained in the case of PPgE2 and PPgE3 results in lower values of molecular weight and polydispersity measured in these cases.

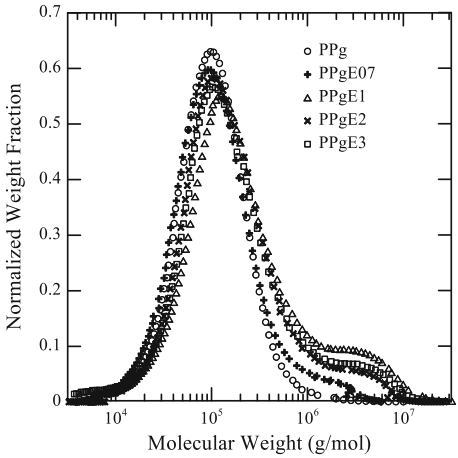

Fig. 4 Molecular weight distribution of all materials

Figure 5 shows the intrinsic viscosity data, [η], as a function of molecular weight obtained with the corresponding SEC detector. These results can be used to evaluate changes in the molecular structure of PPg. Only the data corresponding to PPg, PPgE07 and PPgE1 are displayed since these are the only three materials in which the signal represents the total mass. The figure also includes a straight line corresponding to the prediction of the Mark–Houwink relation, $[\eta] = KM^a$, where M is the molecular weight, and K and a are the Mark–Houwink constants. This relation applies to linear polymers. The fitting of the PPg data to this model results in $a = 0.69$ and $K = 1.74\times10^{-4}$, in agreement with the linear structure of this material. The calculated values are very close to those reported in the literature for linear PP [17, 32]. The intrinsic viscosity data of the modified PPgEs, however, do not follow the Mark–Houwink relation. The data deviate from this relation at high molecular weights (above 200,000 g/mol) and get further apart as the molecular weight increases. This behavior indicates that, for a given molecular weight, the molecules of PPgE07 and PPgE1 are smaller (have smaller radius of gyration) than those of PPg. This can be associated with complex branched structures that have smaller hydrodynamic volume than a corresponding linear one for the same molecular mass [17, 20]. Moreover, the progressive departure of the Mark–Houwink relationship at higher molecular weights indicates that the complexity of the generated structures increases with molecular weight, and it is enhanced with increasing concentration of ER.

In the case of PPgE1, a negative deviation is observed in the whole range of molecular weights of Fig. 5, but a linear trend exists below 200,000 g/mol. This lack of agreement at low molecular weights may be associated with the fact that the value of dn/dc might be changing with the modification of PPg. In fact, small increases, of about 7 and 23%, in the value of dn/dc produces sufficient change in the value of the molecular weight of PPgE07 and PPgE1, respectively, as to obtain superposition of the data with those of PPg in the linear region.

The size of linear and branched polymer molecules in solution is accounted by the classical theory of Zimm and Stockmayer [33, 34]. According to the model of Zimm and Stockmayer, combined with the methodology of Lecachaux [35] the ratio between the mean square radius of gyration of branched molecules and that of the linear material, $g = <S_0^2>_b / <S_0^2>_l$, is related with the ratio of the intrinsic viscosity of these two types of polymers. This relationship is of the form

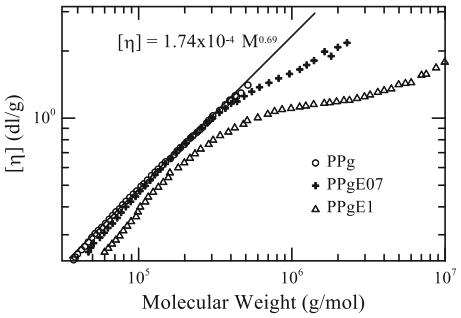

Fig. 5 Intrinsic viscosity of PPg, PPgE07 and PPgE1 as a function of molecular weight

$g^{\varepsilon} = [\eta]_b / [\eta]_l$, where the parameter ε depends on the type of branched structure and the solvent–polymer interaction. It has been suggested that ε has a value of 0.5 for star polymers, 1.5 for combs with large backbones and short branches, and 0.7 for multiarm stars [36–38]. A value of 0.75, which is frequently used for trifunctional random branching [6, 39, 40], was chosen to calculate the average number of branches per macromolecule, m, with:

$$g = \frac{6}{m}\left[\frac{1}{2}\left(\frac{2+m}{m}\right)^{0.5} \ln\left(\frac{(2+m)^{0.5}+m^{0.5}}{(2+m)^{0.5}-m^{0.5}}\right) - 1\right]. \quad (2)$$

This equation is used to compare the molecular structure of the modified polymers even though it is not strictly applicable. The number of branches per 1000 monomer units, N_{LCB}, can be estimated from the average number of branches per macromolecule:

$$N_{\mathrm{LCB}} = 1000 \times M_{\mathrm{M}} \times \frac{m}{M}, \quad (3)$$

where M_{M} is the molar mass of the monomer and M is the molar mass of the branched polymer.

The estimated values of N_{LCB} corresponding to the data in Fig. 5 are shown in Fig. 6. They were calculated using Eq. (3) and parameters $\varepsilon = 0.75$ and $M_{\mathrm{M}} = 42$ g/mol. The branching index increases with the molecular weight in both PPgE07 and PPgE1. The decrease in the value of N_{LCB} of PPgE1 that is observed at large molecular weights may be caused by the retention of the largest molecules by the filtration system. The data in Fig. 6 indicate that PPgE1 presents three times the amount of long branches of PPgE07. The values of N_{LCB} displayed in the figure suggest that PPgE07 and PPgE1, respectively, present approximately 1 and 3 branches every 10^4 carbons, which is the average number of carbons expected in an average PPg molecule. In the analysis of these data, it has to be considered that the position of the AG along the backbone of the PPg molecules is not known and, consequently, the shape of the branched molecules cannot be inferred. Other authors have estimated similar values for synthesized branched PPs using different methods [5, 6, 11, 13, 16, 17, 22].

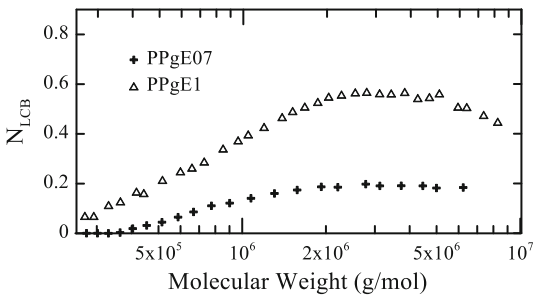

Fig. 6 Estimated number of branches per 1000 monomer units as a function of molecular weight for PPg07 and PPgE1

Linear viscoelastic characterization

Rheological data obtained in the linear viscoelastic regime are particularly helpful to confirm the presence of long-chain branching on polymers. Figures 7 and 8 display, respectively, the elastic modulus, $G'(\omega)$, and dynamic viscosity, $\eta'(\omega) = G''(\omega)/\omega$, of PPg and the polymers modified with ER. PPg exhibits the rheological behavior distinctive of a linear material with low polydispersity and relatively low molecular weight. At high frequencies, where the viscoelastic response is mainly due to the dynamics of short segments of the macromolecules, the dynamic moduli of all materials converge to similar values. On the contrary, at low frequencies, both G' and η' present large changes with respect to the original PPg, being the elastic modulus the one that displays the largest variation with increasing concentration of ER. In particular, the elastic modulus of PPgE3 reaches a value that is approximately four orders of magnitude higher than that of PPg at the lowest frequencies. This behavior, which corresponds to the existence of long relaxation times in the PPgEs, agrees with the increasing complexity of the modified molecules as the concentration of crosslinking agent increases. Moreover, PPgE2 and PPgE3 even display gel-like behavior at low frequencies, with values of G''/G' equal or less to one, respectively.

Figure 8 shows the dynamic viscosity of all the polymers. PPgE07 and PPg display two typical regions: the Newtonian plateau at low frequencies, where the value of viscosity can be considered constant ($\eta' \rightarrow \eta_0$), and the shear-thinning region at high frequencies, where the value of the viscosity decreases with increasing frequency. The materials modified with concentrations of ER greater than 0.7 wt% have higher viscosities with the Newtonian region outside the experimental frequency range. This behavior is typical of topological structures that become gradually more complex as the concentration of the ER is increased. It is interesting to notice that an inflexion point appears in the viscosity curves of the modified polymers at intermediate frequencies. This inflexion point, that is fairly discernible in PPgE07, becomes increasingly noticeable with higher doses of ER.

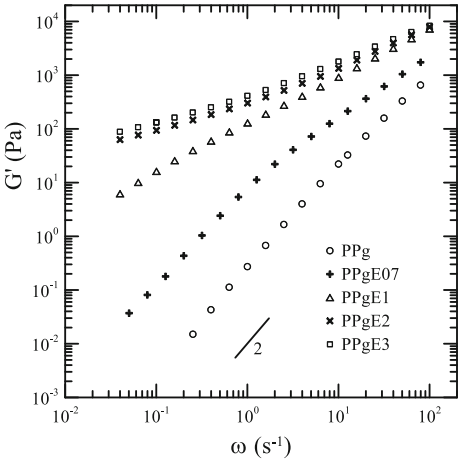

Fig. 7 Elastic modulus of all polymers as a function of frequency at 180 °C

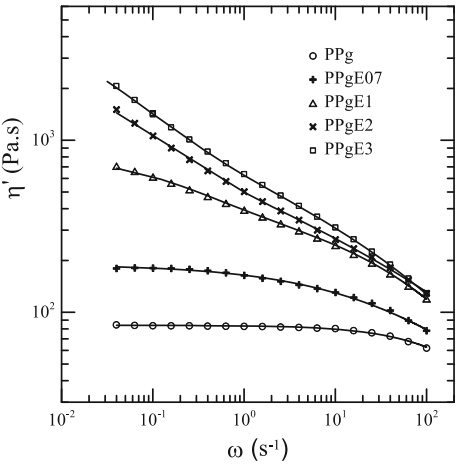

Fig. 8 Dynamic viscosity of all polymers as a function of frequency at 180 °C. *Solid lines*: predictions of the two-mode Cross model [Eq. (4)]

Table 2 Parameters obtained by fitting the two-mode Cross model to the data of Fig. 8

	PPg	PPgE07	PPgE1	PPgE2	PPgE3
η_H (Pa s)	84	145	300	320	410
λ_H (s)	0.0026	0.009	0.023	0.026	0.055
n_H	~0.8	0.7	0.60	0.55	0.55
η_L (Pa s)	–	38	570	3100	5200
λ_L (s)	–	0.77	7	55	80
n_L	–	0.8	0.7	0.65	0.65
η_H/η_L	–	3.8	0.53	0.10	0.079
λ_L/λ_H	–	86	304	2100	1450
η_0 (Pa s)	84	182	870	3420	5610

This behavior, which has been observed in other PPrs and branched systems [14, 22, 25, 41], may be associated with materials that are composed of two distinctive populations of molecules with very different relaxation modes. Considering this observation, the data were then fitted to the two-mode Cross model: [2, 22].

$$\eta*(\omega) = \frac{\eta_H}{1+(\lambda_H\omega)^{n_H}} + \frac{\eta_L}{1+(\lambda_L\omega)^{n_L}} \quad (4)$$

where subscripts H and L stand for high and low frequencies, respectively, and η_i, λ_i and n_i are the corresponding zero-shear viscosity, characteristic relaxation time and shear-thinning index of each of those modes. The predictions of the two-mode Cross model are shown in Fig. 8 with solid lines. These curves were obtained using the adjusted coefficients reported in Table 2. The listed coefficients were obtained by minimum square fitting of the viscosity data. In the case of PPgE2 and PPgE3, the longest relaxation time (λ_L) falls in the limit or even outside the experimental frequency range. To have accurate values of these relaxation times, long creep

experiments should be performed. However, the calculated values are sufficient to analyze the presence of molecular structures having large molecular weight.

As it can be observed, two relaxation modes were needed to obtain a good fitting of the viscosity data of all PPgEs while a single relaxation mode was sufficient in the case of PPg. In the case of the PPgEs, the lowest relaxation time corresponds to the fastest relaxation process (fitting of the high-frequency data) and vice versa. The fastest relaxation process can be related to the relaxation of segments of simple molecular structures, while the slowest one to the relaxation time required by the branched structures and/or higher molecular weight molecules generated by the modification procedure. The parameters reported in Table 2 show that the relaxation time corresponding to high frequencies, λ_H, slightly increase with the concentration of ER, while the one corresponding to low frequencies, λ_L, augments appreciably. In fact, λ_L of PPgE07 is already $\sim$300 times larger than the relaxation time of PPg and the one of PPgE2 is more than four orders of magnitude larger. A similar behavior was observed in a previous study where glycerol was employed as crosslinking agent [22]. In the present work, the synthesized materials present larger ratios of relaxation time, which may be associated with larger levels of long branches. Moreover, as the concentration of ER increases, the first mode gradually loses importance when compared to the new one (η_H/η_L decreases).

From the rheological point of view, it is interesting to perform also a thermo-rheological analysis, since it offers an additional approach to assess the presence of complex molecular structures. Linear polymers have, in general, thermo-rheological simple behavior and obey the time–temperature superposition principle. Figure 9 displays the elastic modulus and the phase angle, $\delta = \tan^{-1}G''/G'$, of PPg, PPgE07 and PPgE1 measured at different temperatures. Only these two PPrs were considered since the rheological behavior of the other PPgEs is surely affected by the gel material. As it may be observed, the distance along the frequency axis between the curves of maximum and minimum temperature of PPgE07 and PPgE1

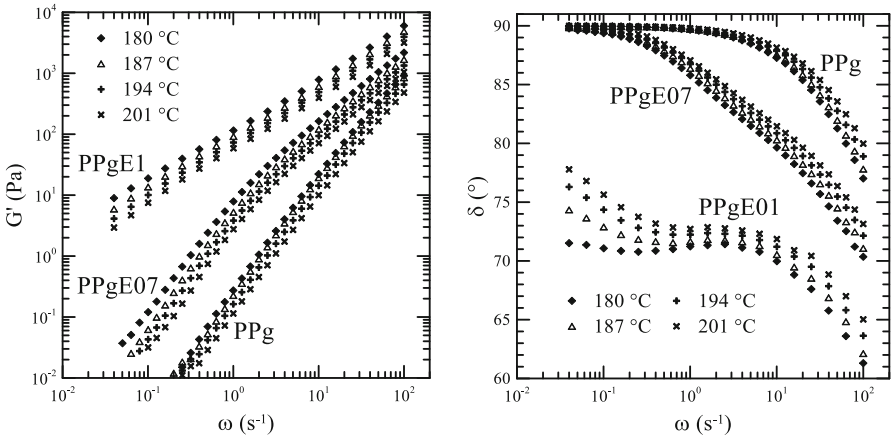

Fig. 9 Elastic modulus (*left*) and phase angle (*right*) of PPg, PPgE07 and PPgE1 measured at different temperatures as a function of frequency

changes with frequency, which does not allow for a unique value of a time–temperature shift factor (a_T) to be applied. Long-branched polymers do not normally obey the time–temperature principle because of the constraints imposed by branching points on chain relaxation. Moreover, branched molecules usually exhibit higher activation energies in the range of frequencies associated with long relaxation times than their equivalent linear counterparts [2, 5, 7, 13, 17, 22, 41–44].

Figure 10 shows the master curves of G', G'' and δ of PPg at the reference temperature of 180 °C (T_0). These master curves were obtained by shifting the curves along the frequency axis, determining the values of a_T for each temperature, and along the y-axis according to factors $b_T = T_0/T$. As it is observed, PPg displays a thermo-rheological simple behavior, typical of a polymer with linear structure, in concordance with SEC measurements. The fitting of the calculated time–temperature shift factors a_T to the Arrhenius model gives an activation energy (E_a) of 39.5 kJ/mol, which is within the range of values reported in the literature for lineal PP [1, 7, 12, 17].

As commented above, PPgE07 and PPgE1 display thermo-rheological complex behavior, given by the failure of the time–temperature superposition principle. Even so, the superposition of data can be attained affecting each data point by a different factor, that is, using an $a_T(\delta)$ [13, 41–44]. Figure 11 shows the master curves of G', G'' and δ of PPgE07 at $T_0 = 180$ °C. The master curve of δ was obtained shifting each data along the frequency axis up to superposition with those at 180 °C, while those of G' and G'' were generated using those same a_T and applying factors b_T to shift the data along the y-axis. As it may be observed, an excellent superposition of the dynamic moduli is achieved using the a_T factors calculated from the phase angle data. Furthermore, this way of presenting the data emphasizes the existence of two populations of structures with different relaxation times.

The values of $a_T(\delta)$ corresponding to PPgE07 were then plotted as a function of $1/T$ to determine the flow activation energy, $E_a(\delta)$, using the Arrhenius model. Figure 12 displays the calculated values. As it can be observed, the activation

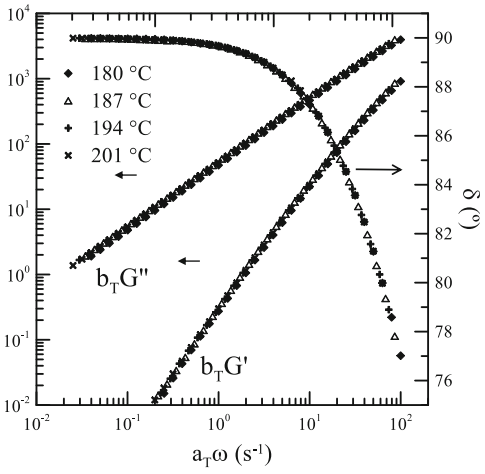

Fig. 10 Master curves of the dynamic moduli and the phase angle of PPg at 180 °C

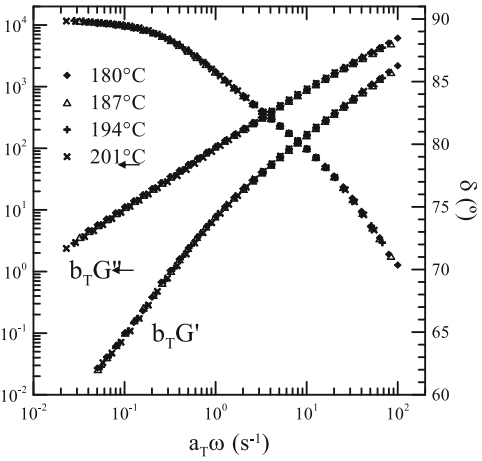

Fig. 11 Master *curves* of the dynamic moduli and the phase angle of PPgE07 at 180 °C

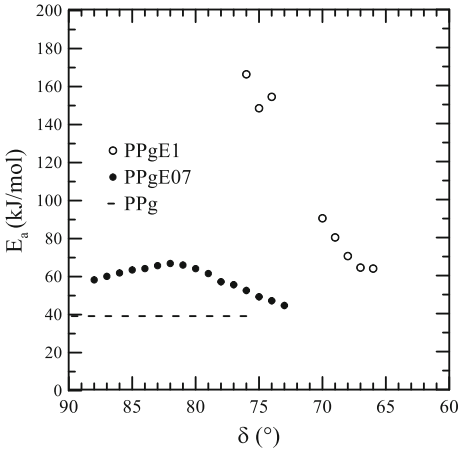

Fig. 12 Activation energy of PPg, PPgE07 and PPgE1 referenced to 180 °C

energy tends to match that of PPg in the high-frequency region (low δ) and is larger at low frequencies ($\delta \rightarrow 90°$), as expected for branched materials. E_a of PPgE07 is almost 50% larger than that of PPg in this range. The complexity of the rheological behavior of PPgE1, which presents a severe S-shaped form in the phase angle curves, allows for the superposition of the data just at the extremes. The values of activation energies of PPgE1 estimated from these data are included in Fig. 12. Although these values most likely are not the exact ones, they indicate that the value of E_a approaches that of PPg at high frequencies and is much larger at low frequencies. Moreover, they also indicate that the difference between the values of activation energies at low and high frequencies increases as the molecular structure becomes more complex.

Thermal analysis

The melting and crystallization behavior of the synthesized materials was analyzed by DSC. The thermograms of PPg and three of the modified polymers, obtained at 10 °C/min, are displayed in Fig. 13. PPgE3 is not included in the figure given the relatively large amount of gel material. Table 3 lists the values of the melting (T_m) and crystallization (T_c) temperatures obtained from the maximum of those thermograms, as well as the onset crystallization temperature ($T_{c,onset}$), the enthalpy of melting (ΔH_m) and crystallization (ΔH_c). These two parameters were calculated from the area of the corresponding peaks. $T_{c,onset}$ was computed as the temperature at which 1 wt% of the material has crystallized.

The fusion of all polymers occurs at about the same temperature range while the crystallization shifts progressively to higher temperature values. All polymers have similar values of T_m and ΔH_m suggesting that, within the degree of modification covered by this work, all the polymers experiment similar melting processes. This is in agreement with other works in the literature that studied the effect of long-chain branching on the thermal properties of polypropylene [14, 15, 19, 21, 22, 25, 26]. Conversely, in the crystallization process, the presence of branching has a more significant effect. The two materials with no evidence of gel, PPgE07 and PPgE1, show one exotherm with a maximum crystallization temperature that shifts from 120 to 127 °C. PPgE2 presents a double exotherm where the first one occurs at a temperature similar to that of PPgE1 and the second exotherm takes place at a lower temperature (see Table 3). Moreover, $T_{c,onset}$ gradually increases with the concentration of crosslinking agent, while ΔH_c is practically constant.

Most works in the literature that analyze the thermal behavior of long-chain branches in PPs have found that T_c increases with respect to lineal PP and gradually augments with the degree of LCBs [8, 14, 19, 21, 28, 45]. This behavior is associated with the nucleating effect of the LCBs. The increase in crystallization

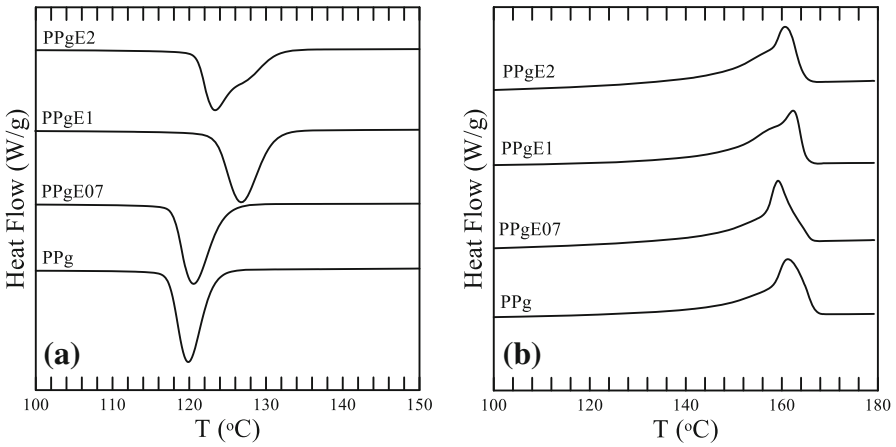

Fig. 13 Thermograms of PPg and modified PPgEs obtained at 10 °C/min during crystallization (**a**) and melting (**b**)

Table 3 Thermal properties of PPg and modified polymers obtained from the thermograms displayed in Fig. 13 obtained at 10 °C/min

	PPg	PPgE07	PPgE1	PPgE2
T_m (°C)	161	159	162	161
ΔH_m (J/g)	105	102	105	102
T_c (°C)	120	121	127	123/128*
ΔH_c (J/g)	101	99	100	99
$T_{c,onset}$ (°C)	125	127	132	132
$t_{1/2}$ (min)	0.50	0.56	0.57	0.75

* Maximum temperatures of the double exotherm

temperature observed in the PPgEs of this work seems to be smaller than in most of the referenced works of the literature. The use of PPg, instead of PP, may be the reason for this difference since the presence of the AGs also has a nucleating effect (T_c of maleic grafted PPs is approximately 7–10 °C larger than that of PP) [46].

To evaluate the effect of changes in molecular structure on the kinetics of the crystallization process, the crystallization enthalpy ratio, χ, was calculated by the accumulative integration of crystallization curves divided by the total crystallization enthalpy, ΔH_c [47]. Figure 14 displays the curves of χ of the four materials corresponding to the thermograms obtained at four cooling rates ($\Phi = 2.5$, 5, 10 and 20 °C/min) as a function of time. This time was calculated as:

$$t = \frac{T_{c,onset} - T}{\Phi}, \tag{5}$$

where T is the temperature and Φ is the cooling rate. The crystallization thermograms obtained at each cooling rate (not shown here) have similar shape and behavior than the ones presented in Fig. 13 at 10 °C/min. Table 4 resumes the corresponding crystallization parameters demonstrating this similarity. It can also be observed that, as expected, increasing the cooling rate in each material produces a shift of T_c and $T_{c,onset}$ towards lower values. A drop of $\sim$10 °C can be appreciated between the values of T_c measured at 2.5 and 20 °C/min for the four compared materials, while a slight reduction is observed in the values of ΔH_c.

The curves of χ(t) in Fig. 14 have all the typical S-shape that corresponds to a nucleation stage followed by crystal growth. As expected, as the cooling rate increases, the crystallization process occurs more rapidly. Figure 14 also shows that the rate of crystallization decreases as the concentration of ER augments. From the curves in Fig. 14, the crystallization half-time, $t_{1/2}$, defined as the time when the material reaches 50% of its crystallization, can be calculated. The values of $t_{1/2}$ are listed in Table 4. At each cooling rate, PPgE07 and PPgE1 display values of $t_{1/2}$ that are slightly larger than the one of PPg, while PPgE2 presents a $t_{1/2}$ that is 50% larger. Moreover, the $t_{1/2}$ of each modified polymer decreases a factor of seven when increasing the cooling rate from 2.5 to 20 °C/min. This phenomenon is typically found in polymer crystallization and occurs because, when increasing the cooling rate, the material requires lower temperatures to crystallize (super-cooling). The increase of the crystallization rate results in a more hindered process, reducing the amount and quality of crystals.

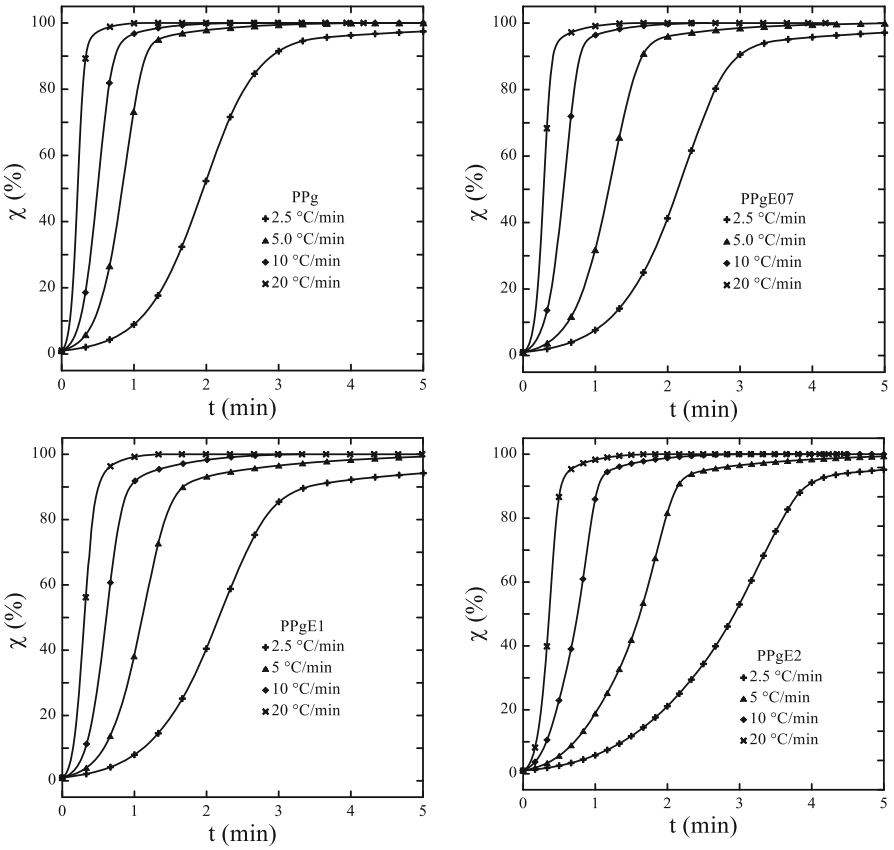

Fig. 14 Crystallization enthalpy ratio of all polymers as a function of time obtained using different cooling rates

Following the approach suggested by Vyazovkin [48], the activation energy of crystallization, ΔE_χ, can be estimated from the χ(t) curves obtained at different cooling rates using:

$$\mathrm{Ln}\left(\frac{\mathrm{d}\chi}{\mathrm{d}t}\right)_\chi = Cte - \frac{\Delta E_\chi}{\mathrm{RT}_\chi}, \tag{6}$$

where $(d\chi/dt)_\chi$ and T_χ are the rate of crystallization and the temperature at a given level of crystallization χ, respectively. The values of ΔE_χ of the four polymers are displayed in Fig. 15. The crystallization activation energy of PPg increases linearly at low values of crystallization enthalpy ratio changing its trend at high χ. In PPgE07 and PPgE1, $-\Delta E_\chi$ decreases linearly in the whole range of χ. It can also be observed that PPg displays the lower crystallization activation energy, which increases with ER concentration up to 1 wt%. PPgE2 also displays a practically linear behavior of ΔE_χ with χ. However, in this case, the data display a larger

Table 4 Thermal properties calculated from the crystallization thermograms obtained at different cooling rates

Material	Φ (°C/min)	T_c (°C)	$T_{c,onset}$ (°C)	$t_{1/2}$ (min)	ΔH_c (J/g)
PPg	2.5	127	132	2.0	103
	5	123	128	0.8	99.6
	10	120	125	0.5	101
	20	117	122	0.2	95.1
PPgE07	2.5	127	132	2.1	99.9
	5	124	130	1.2	99.6
	10	121	127	0.6	98.7
	20	117	123	0.3	97.4
PPgE1	2.5	134	139	2.1	105
	5	130	136	1.1	102
	10	127	132	0.6	100
	20	123	128	0.3	96.6
PPgE2	2.5	130	138	2.9	102.9
	5	127	136	1.6	100.4
	10	123	132	0.8	98.5
	20	119	126	0.4	97.6

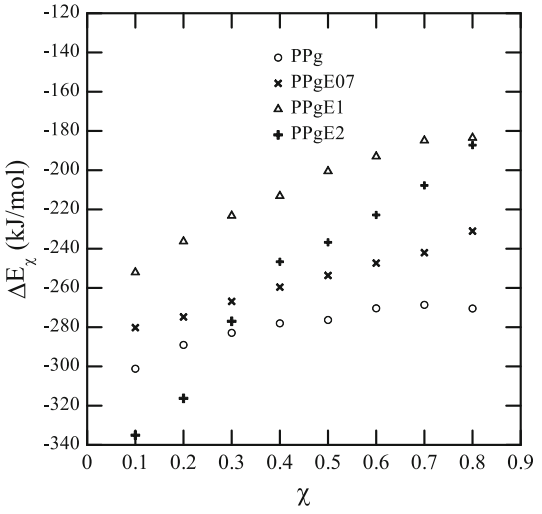

Fig. 15 Crystallization activation energy of as a function of the crystallization enthalpy ratio, for PPg, PPgE07, PPgE1 and PPgE2

dependency with χ than in the other polymers. In fact, at low χ, ΔE_χ is even larger than in PPg.

The observed behavior of the activation energy of crystallization means that nucleation is the controlling mechanism in all polymers except in the case of PPg at high conversion, where diffusion begins to affect the crystallization process

[22, 47, 49]. The value of the activation energy of crystallization of PPg, PPgE07 and PPgE1 suggests that the increasing level of chain branching produces a constraint in the diffusion process. The same behavior was already found when modifying the PPg with different concentrations of glycerol [22]. Moreover, Tian and coworkers [45] calculated a value of $\Delta E_\chi \sim -240$ kJ/mol for long-chain branched PPs at $\chi = 0.2$. In the case of PPgE2, nucleation is also the controlling mechanism. However, in this case, the presence of gel seems to affect the nucleation process, which is more sensitive than in the other polymers to changes in cooling rate at low crystallization enthalpy ratios.

Conclusions

Long-chain branches were generated in a polypropylene grafted with maleic anhydride (PPg) using different concentrations of diglycidyl ether of bisphenol A. The modification process was carried out by reactive mixing in the molten state. According to FTIR analysis, the maleic anhydride groups (AG) in PPg are consumed by the reaction process with the epoxy resin (ER). The amount of AGs rapidly decreases at low concentrations of crosslinking agent (from 0.73 to $\sim$0.43 wt%), while the PPrs obtained with more than about 0.7 wt% of ER display similar amount of unreacted AGs. The inaccessibility of unreacted AGs when one or more of these groups in a PPg molecule have already reacted, and/or a possible phase separation of PPg and ER, may be the cause of the observed behavior. Moreover, the acid groups generated during the modification reaction may participate consuming ER molecules and increasing the crosslinked level.

The generation of more complex molecular structures after the modification process was verified by SEC with triple detectors. The chromatograms of the modified polymers display a bimodal distribution. One population of molecules appears at the same retention volumes than PPg while another, located at lower retention volumes, becomes larger as the concentration of crosslinking agent augments. This population corresponds to new species of molecular weight larger than $\sim$400,000 g/mol. Moreover, the use of the Zimm–Stockmayer model allows estimating that PPgE07 and PPgE1 have about 1 and 3 ramifications per 10^4 carbons, respectively. PPgEs prepared with larger concentrations of ER display traces of gel-like material.

The generated high molecular weight branched molecules strongly affect the viscoelastic properties. The modified materials possess high elasticity and long relaxation modes, with relaxation times and zero-shear rate viscosities that increase with the concentration of crosslinking agent. Moreover, the thermo-rheological behavior of PPgEs is complex. The flow activation energy changes with phase angle and has values much larger than the linear PPg, mainly associated with the large relaxation processes.

The presence of branches in the molecular structure of PPg also affects the crystallization process of the polymer, mainly the activation energy of crystallization which increases with the degree of modification of PPg. Nucleation is the

controlling mechanism in the case of the PPgEs in the whole range of crystallization enthalpy ratio.

Acknowledgements The authors are grateful for the financial support given by the National Research Council of Argentina (CONICET), the Universidad Nacional del Sur (UNS), the Agencia Nacional de Promoción Científica y Tecnológica (ANPCyT) and the CYTED Project 311RT0417.

References

1. Gahleitner M (2001) Melt rheology of polyolefins. Prog Polym Sci 26:895–944
2. Han CD (2007) Rheology and Processing of Polymeric Materials, Polymer Rheology, vol 1. Oxford University Press, New York
3. Utracki LA (2002) Polymer blends handbook, vol 1. Kluwer Academic Publisher, Berlin
4. Lu B, Chung TC (1999) Synthesis of long chain branched polypropylene with relatively well-defined molecular structure. Macromolecules 32:8678–8680. doi:10.1021/ma991010r
5. Sugimoto M, Tanaka T, Masubuchi Y, Takimoto JI, Koyama K (1999) Effect of chain structure on the melt rheology of modified polypropylene. J Appl Polym Sci 73:1493–1500. doi:10.1002/(SICI)1097-4628(19990822)73:8<1493:AID-APP18>3.0.CO;2-2
6. Lagendijk RP, Hogt AH, Buijtenhuijs A, Gotsis AD (2001) Peroxydicarbonate modification of polypropylene and extensional flow properties. Polymer 42:10035–10043. doi:10.1016/S0032-3861(01)00553-5
7. Rätzsch M, Arnold M, Borsig E, Ra M, Bucka H, Reichelt N (2002) Radical reactions on polypropylene in the solid state. Prog Polym 27:1195–1282. doi:10.1016/S0079-6700(02)00006-0
8. Graebling D (2002) Synthesis of branched polypropylene by a reactive extrusion process. Macromolecules 35:4602–4610. doi:10.1021/ma0109469
9. Auhl D, Stange J, Münstedt H, Krause B, Voigt D, Lederer A, Lappan U, Lunkwitz K (2004) Long-chain branched polypropylenes by electron beam irradiation and their rheological properties. Macromolecules 37:9465–9472. doi:10.1021/ma030579w
10. Auhl D, Stadler FJ, Münstedt H (2012) Comparison of molecular structure and rheological properties of electron-beam- and gamma-irradiated polypropylene. Macromolecules 45:2057–2065. doi:10.1021/ma202265w
11. Gotsis AD, Zeevenhoven BLF, Hogt AH (2004) The effect of long chain branching on the processability of polypropylene in thermoforming. Polym Eng Sci 44:973–982. doi:10.1002/pen.20089
12. Paavola S, Saarinen T, Löfgren B, Pitkänen P (2004) Propylene copolymerization with non-conjugated dienes and α-olefins using supported metallocene catalyst. Polymer 45:2099–2110. doi:10.1016/j.polymer.2004.01.053
13. Ye Z, AlObaidi F, Zhu S (2004) Synthesis and rheological properties of long-chain-branched isotactic polypropylenes prepared by copolymerization of propylene and nonconjugated dienes. Ind Eng Chem Res 43:2860–2870. doi:10.1021/ie0499660
14. Nam GJ, Yoo JH, Lee JW (2005) Effect of long-chain branches of polypropylene on rheological properties and foam-extrusion performances. J Appl Polym Sci 96:1793–1800. doi:10.1002/app.21619
15. Krause B, Voigt D, Häußler L, Auhl D, Münstedt H (2006) Characterization of electron beam irradiated polypropylene: influence of irradiation temperature on molecular and rheological properties. J Appl Polym Sci 100:2770–2780. doi:10.1002/app.23453
16. Tian J, Yu W, Zhou C (2006) The preparation and rheology characterization of long chain branching polypropylene. Polymer 47:7962–7969. doi:10.1016/j.polymer.2006.09.042
17. Langston JA, Colby RH, Chung TCM, Shimizu F, Suzuki T, Aoki M (2007) Synthesis and characterization of long chain branched isotactic polypropylene via metallocene catalyst and t-reagent. Macromolecules 40:2712–2720. doi:10.1021/ma062111+
18. Fina A, Tabuani D, Peijs T, Camino G (2009) POSS grafting on PPgMA by one-step reactive blending. Polymer 50:218–226. doi:10.1016/j.polymer.2008.11.002
19. Li S, Xiao M, Wei D, Xiao H, Hu F, Zheng A (2009) The Melt grafting preparation and rheological characterization of long chain branching polypropylene. Polymer 50:6121–6128. doi:10.1016/j.polymer.2009.10.006

20. Mabrouk KE, Parent JS, Chaudhary BI, Cong R (2009) Chemical modification of PP architecture: strategies for introducing long-chain branching. Polymer 50:5390–5397. doi:10.1016/j.polymer.2009.09.066
21. Su F, Huang H (2009) Rheology and thermal behavior of long branching polypropylene prepared by reactive extrusion. J Appl Polym Sci 113:2126–2135. doi:10.1002/app.30061
22. Guapacha J, Failla MD, Vallés EM, Quinzani LM (2014) Molecular, rheological, and thermal study of long-chain branched polypropylene obtained by esterification of anhydride grafted polypropylene. J Appl Polym Sci 131:40357. doi:10.1002/app.40357
23. Hingmann R, Marczinke BL (1994) Shear and elongational flow properties of polypropylene melts. J Rheol 38:573–587. doi:10.1122/1.550475
24. Zhang C, Niu H, Dong JY (2012) Fabrication of long chain branched polypropylene using click chemistry. Polym Bull 68:949–959. doi:10.1007/s00289-011-0588-7
25. Yoshiga A, Otaguro H, Parra DF, Lima LFCP, Lugao AB (2009) Controlled degradation and crosslinking of polypropylene induced by gamma radiation and acetylene. Polym Bull 63:397–409. doi:10.1007/s00289-009-0102-7
26. Oliani WL, Parra DF, Lima LFCP, Lugao AB (2012) Morphological characterization of branched PP under stretching. Polym Bull 68:2121–2130. doi:10.1007/s00289-012-0708-z
27. Zhang W, Yang L, Chen P, Zhang H, Lin W, Wang Y (2013) Preparation of long-chain branching polypropylene and investigation on its foamability. Polym Eng Sci 53:1598–1604. doi:10.1002/pen.23416
28. Tang H, Dai W, Chen B (2008) A new method for producing high melt strength polypropylene with reactive extrusion. Polym Eng Sci 48:1339–1344. doi:10.1002/pen.21105
29. Chaudhary BI, Cong R, Parent JS (2011) Imide-coupled propylene-based polymer and process. Patent US 2011/0009513 A1
30. Ashcroft WR (1993) Curing agents for epoxy resins. Chemistry and Technology of Epoxy Resins. Springer, The Netherlands, pp 37–71
31. Silverstein R, Webster F (1991) Spectrometric identification of organic compounds, 5th edn. Wiley, New York
32. Scholte TG, Meijerink NLJ, Schoffeleers HM, Brands AMG (1984) Mark-Houwink equation and GPC calibration linear short-chain branched polyolefins, including polypropylene and ethylene-propylene copolymers. J Appl Polym Sci 29:3763–3782. doi:10.1002/app.1984.070291211
33. Zimm BH, StocKmayers WH (1949) The dimensions of chain molecules containing branches and rings. Chem Phys 17:1301–1314. doi:10.1063/1.1747157
34. Zimm BH, Kilb RW (1959) Dynamics of branched polymer molecules in dilute solution. J Polym Sci 37:19–42. doi:10.1002/pol.1959.1203713102
35. Lecacheux D, Lesec J, Quivoron C (1982) High-temperature coupling of high-speed GPC with continuous viscometry. I. Long-chain branching in polyethylene. J Appl Polym Sci 27:4867–4877. doi:10.1002/app.1982.070271231
36. Berry GCJ (1971) Thermodynamic and conformational properties of polystyrene. III dilute solution studies on branched polymers. J Polym Sci Part A-2 9:687–715
37. Roovers J, Toporowski P, Martin J (1989) synthesis and characterization of multiarm star polybutadienes. Macromolecules 22:1897–1903. doi:10.1021/ma00194a064
38. Wood-Adams P, Dealy JM, de Willem Groot A, Redwine OD (2000) Effect of molecular structure on the linear viscoelastic behavior of polyethylene. Macromolecules 33:7489–7499. doi:10.1021/ma991533z
39. Zhang Z, Wan D, Xing H, Tan H, Wang L, Zheng J, An Y, Tang T (2012) A new grafting monomer for synthesizing long chain branched polypropylene through melt radical reaction. Polymer 53:121–129. doi:10.1016/j.polymer.2011.11.033
40. Li Y, Yao Z, Chen Z, Qiu S, Zeng C, Cao K (2013) Rheological evidence of physical cross-links and their impact in modified polypropylene. Ind Eng Chem Res 52:7758–7767. doi:10.1021/ie400809z
41. Vega JF, Expósito MT, Martínez-Salazar J, Lobón-Poo M, Osío Barcina J, García Martínez A, López M (2011) Molecular architecture and linear viscoelasticity of homogeneous ethylene/styrene copolymers. Rheol Acta 50:207–220. doi:10.1007/s00397-010-0521-2
42. Villar MA, Failla MD, Quijada R, Santos Mauler R, Vallés E, Barrera Galland G, Quinzani LM (2001) Rheological characterization of molten ethylene-alfa-olefin copolymers synthesized with Et [Ind] 2 ZrCl 2/MAO catalyst. Polymer 42:9269–9279. doi:10.1016/S0032-3861(01)00458-X
43. Wood-Adams P, Costeux S (2001) Thermorheological behavior of polyethylene: effects of microstructure and long chain branching. Macromolecules 34:6281–6290. doi:10.1021/ma0017034

44. Keßner U, Münstedt H (2010) Thermorheology as a method to analyze long-chain branched polyethylenes. Polymer 51:507–513. doi:10.1016/j.polymer.2009.11.005
45. Tian J, Yu W, Zhou C (2007) Crystallization behaviors of linear and long chain branched polypropylene. J Appl Polym Sci 104:3592–3600. doi:10.1080/00222340600870507
46. Seo Y, Kim J, Ung K, Chul Y (2000) Study of the crystallization behaviors of polypropylene and maleic anhydride grafted polypropylene. Polymer 41:2639–2646. doi:10.1016/S0032-3861(99)00425-5
47. Kang J, Wang B, Peng H, Chen J, Cao Y, Li H, Yang F, Xiang M (2014) Investigation on the structure and crystallization behavior of controlled-rheology polypropylene with different stereo-defect distribution. Polym Bull 71:563–579. doi:10.1007/s00289-013-1077-y
48. Vyazovkin S (2002) Is the Kissinger equation applicable to the processes that occur on cooling? Macromol Rapid Commun 23:771–775. doi:10.1002/1521-3927(20020901)23:13<771:AID-MARC771>3.0.CO;2-G
49. Yang B, Yang M, Wang WJ, Zhu S (2012) Effect of long chain branching on nonisothermal crystallization behavior of polyethylenes synthesized with constrained geometry catalyst. Polym Eng Sci 52:21–34. doi:10.1002/pen.22040